Amino Acids (2012) 43:557–565
DOI 10.1007/s00726-011-1150-5

ORIGINAL ARTICLE

Molecular dynamics simulation exploration of unfolding and refolding of a ten-amino acid miniprotein

Guang-Jiu Zhao · Chang-Li Cheng

Received: 1 July 2011 / Accepted: 4 November 2011 / Published online: 24 November 2011

Abstract Steered molecular dynamics simulations are performed to explore the unfolding and refolding processes of CLN025, a 10-residue beta-hairpin. In unfolding process, when CLN025 is pulled along the termini, the force-extension curve goes back and forth between negative and positive values not long after the beginning of simulation. That is so different from what happens in other peptides, where force is positive most of the time. The abnormal phenomenon indicates that electrostatic interaction between the charged termini plays an important role in the stability of the beta-hairpin. In the refolding process, the collapse to beta-hairpin-like conformations is very fast, within only 3.6 ns, which is driven by hydrophobic interactions at the termini, as the hydrophobic cluster involves aromatic rings of Tyr1, Tyr2, Trp9, and Tyr10. Our simulations improve the understanding on the structure and function of this type of miniprotein and will be helpful to further investigate the unfolding and refolding of more complex proteins.

Keywords Protein folding · Protein unfolding · Hydrogen bond · Beta-hairpin · Steered molecular dynamics

Introduction

It is well known that most proteins are functional in vivo because they fold into characteristic three-dimensional structures (George et al. 2006). Under some conditions, such as high temperature, extremes of pH or mechanical forces, protein will unfold into random coil that loses biochemical function (Selkoe 2003). Since folding and unfolding are essential to life, literatures on the study of these processes are very rich (Gao and Truhlar 2002; Gao et al. 2006; Freddolino et al. 2010; Yang et al. 2010; Alhambra et al. 2000; Duan et al. 2010; Shank et al. 2010). And it has been greatly advanced in recent years by the development of fast time-resolved techniques. For instance, an atomic force microscope (AFM) can be used to study unfolding by attaching one end of a protein to a substrate and the other end to the AFM's cantilever. It enables the characterization of the mechanical response of protein at the nanometer scale (Sotomayor and Schulten 2007; Best et al. 2003). Moreover, two-dimensional infrared (2D IR) spectroscopy, which maps vibrational coupling between molecular groups, can be used to probe protein folding and unfolding dynamics with picosecond time resolution (Golonzka et al. 2001; Hunt 2009; Kolano et al. 2006; Ganim et al. 2008). Hydrogen-exchange mass-spectrometry can track the formation of secondary structures during folding by measuring how easily protons (H^+ ions) are exchanged between water and amino acids in the proteins (Tsui et al. 1999; Eyles and Kaltashov 2004; Pan et al. 2010; Chen et al. 2010; Gruebele 2010). However, a detailed understanding of folding is still missing due to the high dimensionality of the protein conformational spaces and by the wide range of relevant time scales (Daniel et al. 2003).

In order to reduce complexity, a large amount of works have been concentrated on protein secondary structure conformational dynamics, such as β-hairpin (Munoz et al. 2006; Hughes and Waters 2006; Riemen and Waters 2010; Klimov et al. 2002; Zhou and Berne 2002; Guo et al. 2000; Du et al. 2004). Schulten et al. perform flow simulations on

G.-J. Zhao (✉) · C.-L. Cheng
State Key Laboratory of Molecular Reaction Dynamics, Dalian Institute of Chemical Physics, Chinese Academy of Sciences, 457 Zhongshan Road, Dalian 116023, China
e-mail: gjzhao@dicp.ac.cn

the 16-residue β-switch region of platelet glycoprotein Ibα (Chen et al. 2008). The flow induces its transition from a flexible loop to a β-hairpin. Among so many synthesized β-hairpins, photo-switchable peptide is the most popular. It incorporates a photoresponsive element which can initiate structural changes from a β-hairpin to an unfolded hydrophobic cluster and vice versa. Moroder et al. have synthesized various peptides, in which an azobenzene unit was incorporated directly in the backbone (Renner et al. 2000a, b; Cattani-Scholz et al. 2002). An optical laser pulse excites the molecular system and then azobenzene will perform cis–trans photoisomerization, which cause subsequent conformational dynamics of the peptide backbone (Nguyen and Stock 2006; Olsen and Smith 2007, 2008; Spörlein et al. 2002).

Since miniproteins play an important role in the study of protein folding, numerous β-hairpin miniproteins have been designed recently. Honda et al. (2008) obtained the crystal structure of a β-hairpin miniature protein, termed CLN025, which is a synthetic molecule consisting of 10 naturally occurring amino acids. The linear sequence of amino acids of CLN025 is Tyr1-Tyr2-Asp3-Pro4-Glu5-Thr6-Gly7-Thr8-Trp9-Tyr10 (see Fig. 1). The β-hairpin is stabilized by an electrostatic interaction between the charged termini; cross-strand hydrogen bonds; Ar–Ar interactions between Tyr2 and Trp9, Tyr1 and Tyr10, Tyr1 and Trp9, and Tyr2 and Tyr10; as well as a CH–π interaction between Try2 and Pro4. Despite its small size, its essential characteristics, revealed by its crystal structure, solution structure, thermal stability and free energy surface are consistent with the properties of natural proteins.

The existence of this kind of miniprotein deepens our understanding of natural proteins. However, we have known little about the details of folding and unfolding process for CLN025 yet. In this paper, we study the unfolding of CLN025 by mechanical stretching using steered molecular dynamics (SMD) simulation, which mimics AFM experiment and reveals the molecular mechanisms underlying mechanical function (Guzmán et al. 2008, 2009; Lu and Schulten 1999; Hamdi et al. 2008; Rief et al. 1997; Lim et al. 2008; Zeng et al. 2010). Because of computational limits, the pulling velocities used in SMD are orders of magnitude higher than those in an AFM experiment, leading to drastic overestimation of the unfolding forces. However, the resulting force-extension profiles can illustrate qualitative details that are consistent with those observed by AFM (Gao and Truhlar 2002; Lu and Schulten 2000). Furthermore, we also simulate the refolding of stretched CLN025 by free MD simulation.

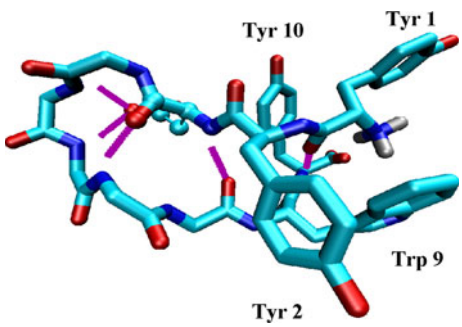

Fig. 1 Crystal structure of CLN025. The β-hairpin is stabilized by the hydrogen bonds and hydrophobic interaction between nonpolar side chains of Tyr1 and Tyr10, Tyr2 and Trp9

Theoretical methods

Simulations were performed with the molecular dynamics code NAMD 2.7 with the CHARMM27 force field (Phillips et al. 2005). The protein was solvated in a rectangle box of $5.9 \times 4.8 \times 4.1$ nm^3. One chloride and three sodium ions were used to neutralize the charge of the system. An energy minimization of 1,000 steps using the steepest descent algorithm was followed by a 1-ns position-constrained NPT simulation in order to equilibrate water and ions. A subsequent NPT simulation of 10 ns was performed with the peptide released. The temperature ($T = 310$ K) and pressure ($p = 1$ bar) were controlled by langevin thermostats and barostats. The bonds were constrained using the Shake method in all simulations. The simulation utilized particle mesh Ewald summation with a 12-Å cutoff for nonbonding interactions and an integration step of 2 fs (Pineda et al. 2007; Saen-Oon et al. 2008; Cramer and Truhlar 1999; Wu et al. 2007; Huang et al. 2008; Liu et al. 2009; Zhao et al. 2010; Yang et al. 2011).

For the steered MD simulations, constant velocity SMD method was used to stretch peptides along two ends of the protein. In this technique virtual harmonic force is applied to the Cα atom of Tyr10, with the N atom of Tyr1 fixed simultaneously. The force constant of Hookean spring is 7 kcal mol^{-1} Å^{-2}. The pulling velocity is 0.01 Å ps^{-1}. For comparison, we have performed another unfolding pathway simulation. We attach a spring at the Cα atom of residue Gly7 while the Cα atom of residue Asp3 is held fixed (Li et al. 2009). It helps us to study how much the attraction between two termini contributes to the stability of the β-hairpin structure. Moreover, we have also done the simulations in vacuum in order to study the role of water in unfolding of CLN025.

Results and discussion

The stable structure of CLN025 is obtained after a 10-ns free MD simulation at 310 K and compared with the

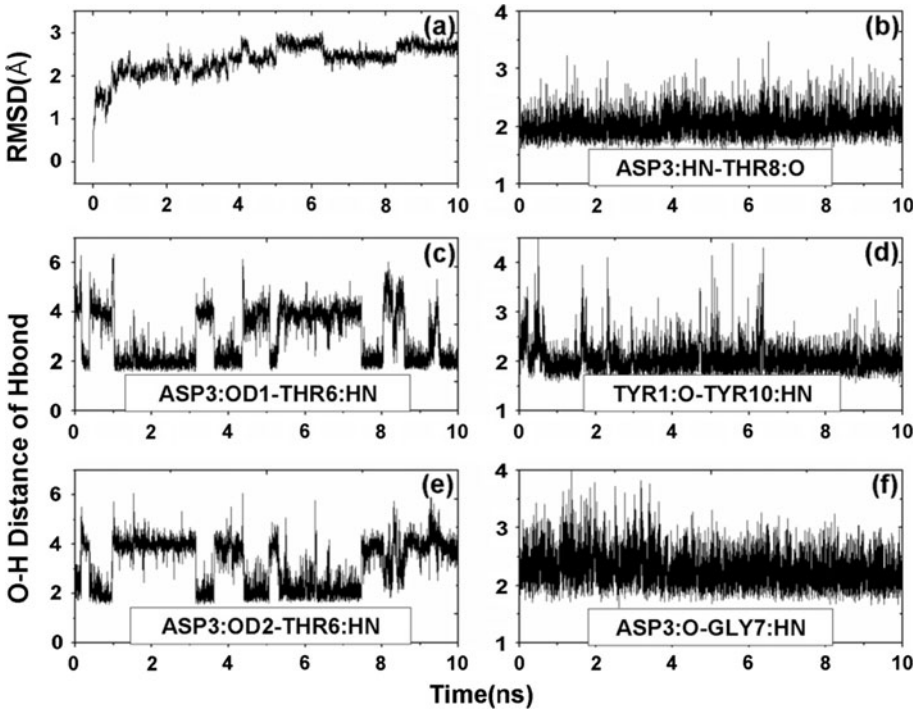

Fig. 2 Equilibration dynamics of CLN025. **a** Time course of the RMSD of MD structures ($T = 310$ K) from NMR structure. **b–f** O–H distance of the backbone H-bonds versus time during the 10 ns equilibration. We use the five cross-strand H-bond distances as key quantities for monitoring conformational dynamics as well as stability along the trajectory. Other H-bonds do not survive more than 20% of overall simulation time

crystal structure. The stability of the used structure can be reflected by the small and constant overall root mean square displacement (RMSD) values (2.4 ± 0.6 Å) after 500 ps (see Fig. 2a). We also calculate the average RMSD over time of each residue in the protein with the VMD software package (Humphrey et al. 1996). The most mobile residues are Tyr10 and Trp9, with average RMSD value being 3.81 and 2.67 Å, respectively. The most stable residues are Glu6 and Tyr7, whose average RMSD values are both 0.89 Å. Trp9 and Tyr10 are mobile for the reason that they both incorporate an aromatic sidechain so that many rotamers are possible.

The oxygen hydrogen (O–H) distances of the interstrand backbone H-bonds are presented in Fig. 2b–f. We use the five cross-strand H-bond distances as key quantities for monitoring conformational dynamics as well as stability along the trajectory. The diagrams show that there are only three stable hydrogen bonds, i.e. Asp3: NH···O: Thr8, Tyr1: O···HN: Tyr10, Asp3: O···HN: Gly7. In addition, Asp3: OD1 and Asp3: OD2 can form hydrogen bond with HN: Thr6 alternately. The other hydrogen bonds can last less than 20% of the equilibration duration time.

Then, SMD simulation has been performed with the equilibration structure. Figure 3a represents the force extension profile when pulling force is along the N-terminus and C-terminus during the unfolding process. It is observed that the force fluctuates between negative and positive values after 0.2 ns, which means that it is easy to be unraveled along the terminal direction. The phenomenon is very different from what happens in other peptides, where force is always positive. As the C-terminus detaches from the N-terminus, stable hydrogen bonds break soon by continuous attacks from water molecules (Rhee et al. 2004; Li et al. 2010; Shelimov et al. 1997).

The unfolding sequence can be well explained by the study of change in the interaction energy between different residues (Hatfield et al. 2010; Das and Mukhopadhyay 2009). From Fig. 3b, it can be noted that major contribution to the interaction energy is from Asp3-Thr6 and Tyr1-Tyr10. Other interaction energies are far less than the above two and are not shown. One can also see that the interaction energy from Tyr1-Tyr10 significantly changes within 0.11 ns and disappears after another 0.25 ns. The H-bond between Asp3 and Thr6 is not stable and broken after 0.36 ns.

Figure 3c shows the extension profile of constant stretching force simulation with force being 100 pN. It demonstrates a clear three-phase process. In phase I, the extension varies around 4.6 Å, corresponding to terminal attraction's resistance. In phase II, the protein extends rapidly from 4.6 to 23 Å, without much resistance. In phase III, the plateau region is observed to form a distinct hyper-unfolded state in which the central kink of the hairpin is straightened (Bryant et al. 2000). As mentioned above, the β-hairpin can unfold easily without large barrier in the unfolding process when pulling is along the termini. This demonstrates that the β-hairpin is dominantly stabilized by the electrostatic interaction between the charged termini.

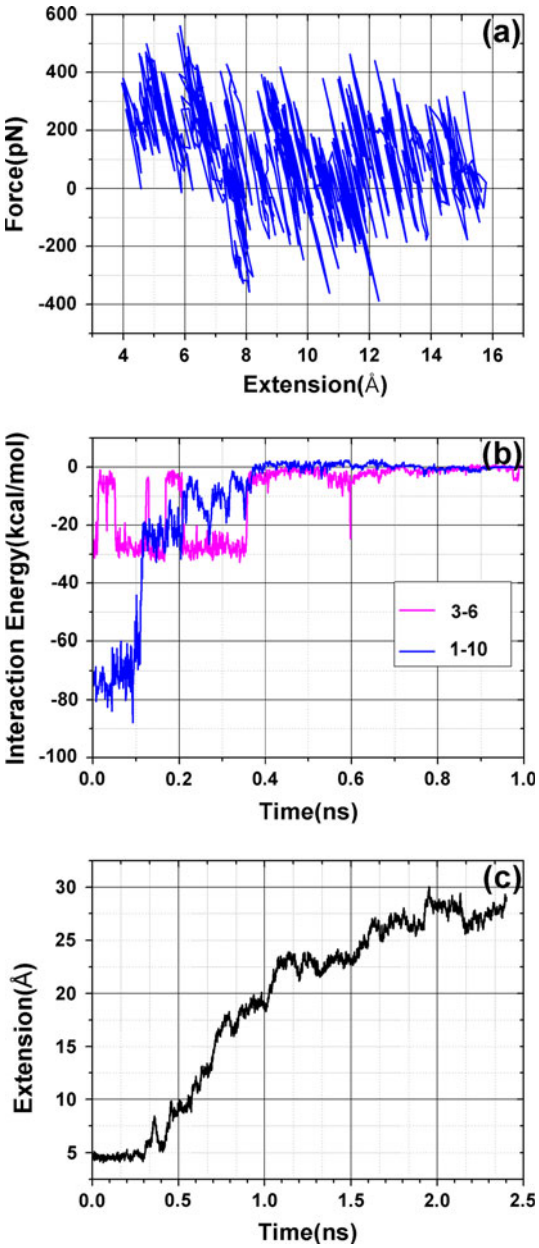

Fig. 3 Mechanical unfolding of CLN025 in aqueous solution when pulled from the termini. **a** Force-extension curve of a 1.6 ns constant velocity SMD simulation. Not long after the beginning of the simulation, the force fluctuates between negative and positive values, which means that it is easy to be unraveled along the terminal direction. **b** Interaction energy between different residues along the unfolding pathway in (**a**). Only the important ones are shown. "*3–6*" means interaction energy between residue Asp3 and Thr6. **c** Constant force simulation (100 pN). CLN025 only resists for 0.4 ns. The plateau at the end represents that protein becomes completely unfolded

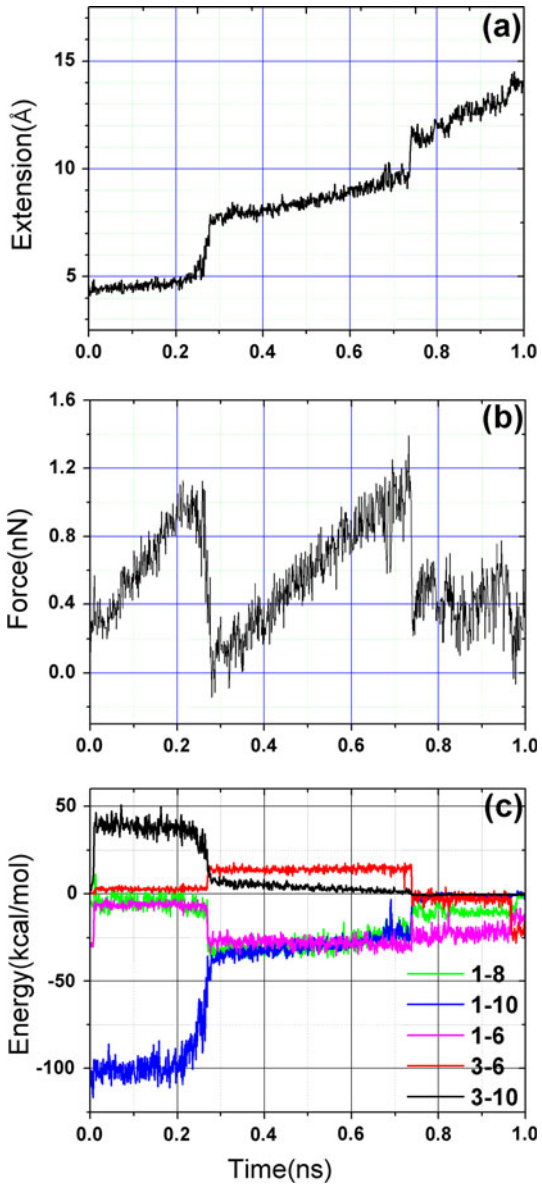

Fig. 4 Mechanical unfolding of CLN025 in gas phase when pulled from the termini. Data shown are time evolution of (**a**) extension, (**b**) force, (**c**) interaction energy, respectively. A sudden jump of the extension corresponding to force and interaction energy's sharp decrease

Mechanical unfolding process of CLN025 in gas phase when it is pulled from the termini is shown in Fig. 4. A sudden jump of the extension corresponds to a sharp decrease of force and interaction energy. There are two clear force peaks in Fig. 4a, which is different from that in aqueous solution. One can observe that hydrogen bonds can survive for a much longer time with the absence of water. And the interaction energy between Tyr1 and Tyr10 also increases from 75 to 100 kcal/mol.

Moreover, we perform SMD simulations from the middle residues: the α carbon of Asp3 is held fixed while that of Gly7 is harmonically constrained to a moving restraint point. Two collective variables, radius of gyration

(Rg) of the core and the number of hydrogen bonds are calculated from the molecular structures along the unfolding pathway. Rg is defined as the root mean square distance of the four aromatic sidechain atoms of the hydrophobic core Tyr1, Tyr2, Trp9, and Tyr10 residues from their collective center of mass. The number of hydrogen bonds is calculated by counting the number of donor–acceptor pairs in which the distance between N and O is less than 3 Å and the angle N–H···O is larger than 130°.

The Force–time curve is overlaid with plots of the number of hydrogen bonds and the radius of gyration of the hydrophobic core sidechains in Fig. 5. There are two main force peaks, which are marked by black rows. The first force peak indicates the resistance of hydrogen bonds, the number of which drops from 9 to 4 within 0.3 ns. The second force peak represents the resistance of hydrophobic core, as can be seen by the rise in the radius of gyration of the core following the force peak.

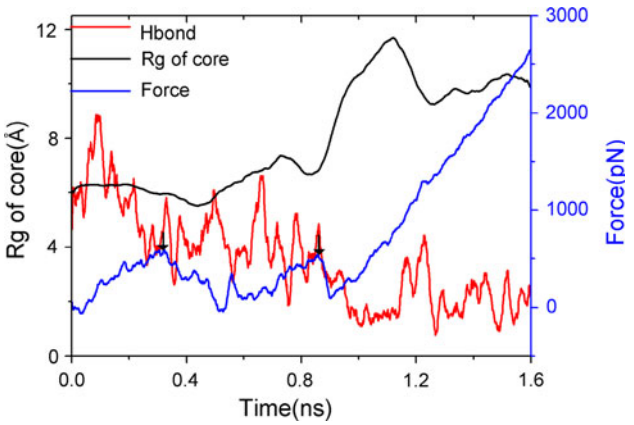

Fig. 5 Unfolding pathway of the β-hairpin when pulled from middle residues in aqueous solution. Force–time curves are overlaid with plots of the number of hydrogen bonds and the radius of gyration of the hydrophobic core sidechains. All traces have been smoothed by boxcar averaging

Figure 6 depicts molecular dynamics snapshots of the unfolding pathway when we pull along the middle residues. Compared with snapshots in aqueous solution, the C-terminus does not detach from the N-terminus during the whole simulation time in vacuum. In aqueous solution, the three hydrogen atoms of N-termini may form hydrogen bond with three surrounding water molecules while in vacuum, the N-termini is hidden in the innerside of the β-switch and forms hydrogen bonds with Asp3 and Thr6. Either pulled from the terminal or middle residues, the β-hairpin unfolds slower in vacuum than in aqueous solution because enhanced electrostatic interactions at the terminal positions of the peptide can contribute to the stability of the β-hairpin.

Since a two-state kinetic model of protein folding is valid, (Zwanzig 1997) it would be tested by time evolution of the backbone dihedral angles (Fig. 7). Transition from folded state to unfolded state will be accompanied by sudden change of backbone dihedral angles. Regardless at which site we pull the β-hairpin in aqueous solution, at the terminal or at middle residues, its final backbone dihedral angles are the same, which is shown in Table 1.

To study the refolding of CLN025, we perform molecular dynamics simulations starting from a partially unfolded state. Figure 8a is the RMSD of MD structures from crystal structure. The collapse to β-hairpin-like

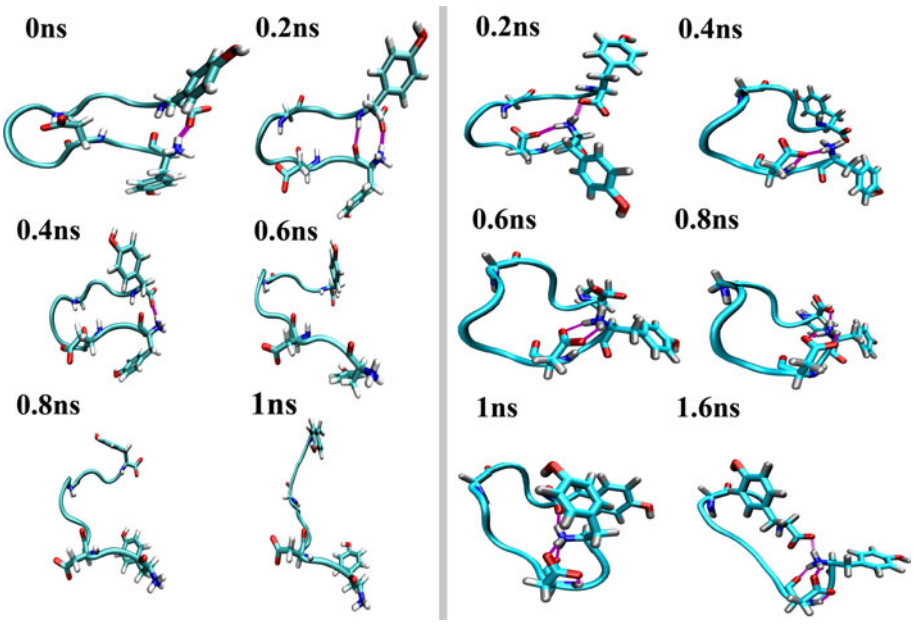

Fig. 6 Molecular dynamics snapshots demonstrating the unfolding pathway under tension applied at the middle residues. In aqueous solution (*left*) and in vacuum (*right*). Compared with snapshots in aqueous solution, the C-terminus does not detach from the N-terminus through the whole simulation time in vacuum

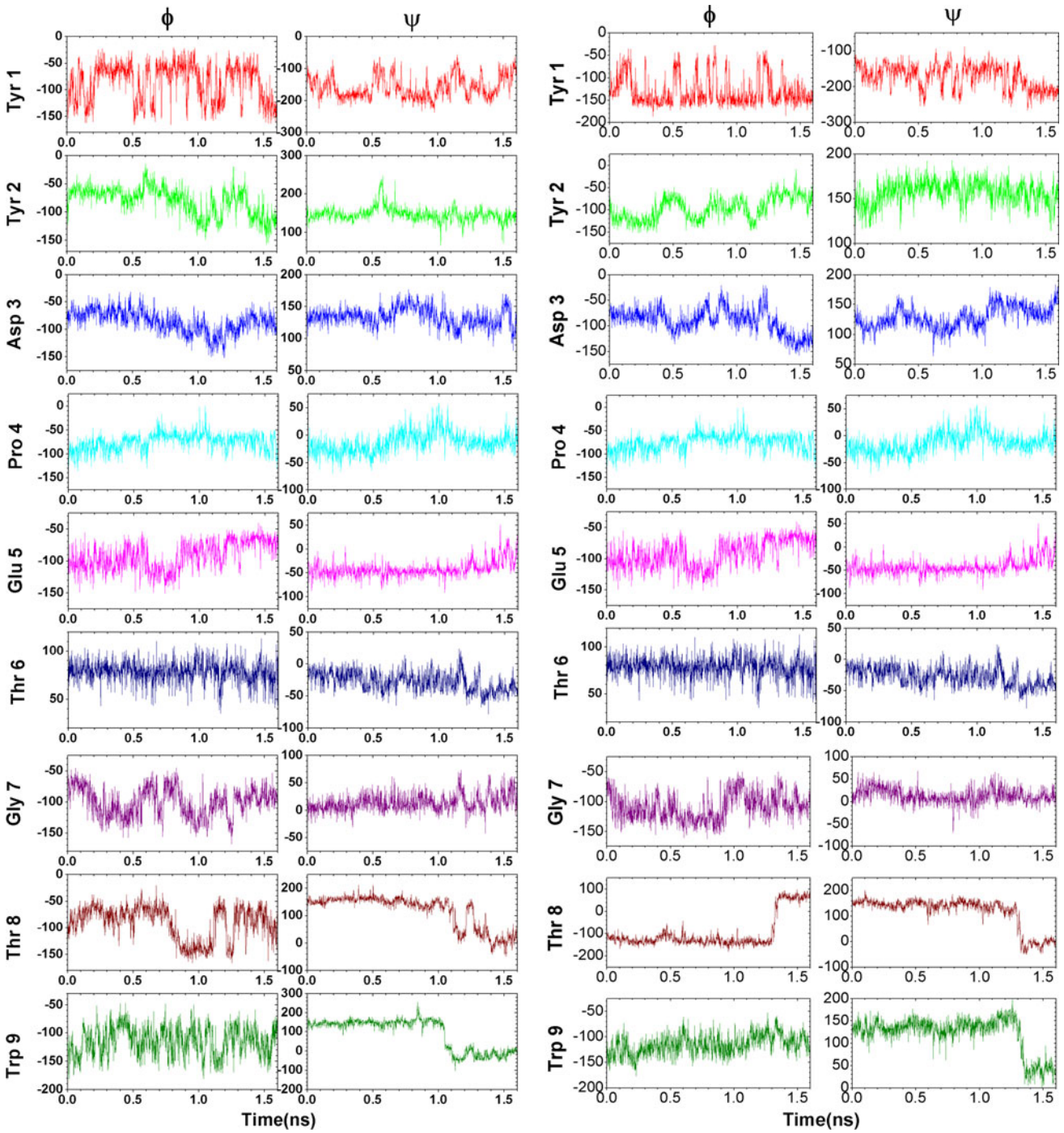

Fig. 7 Time evolution of the backbone dihedral angles Φ_i (t) and Ψ_i (t) of the ten amino acids of CLN025 when pulled from termini (*left*); pulled from middle residues (*right*). Φ_i involves the backbone atoms C_i–N_{i+1}–$C\alpha_{i+1}$–C_{i+1}. Ψ_i involves the backbone atoms N_i–$C\alpha_i$–C_i–N_{i+1}

conformations is very fast, with only 3.6 ns. Then the 10-residue peptide stays in folded state until 20 ns. The reason why it refolds rapidly is that in initial structure, the turn has not been disrupted thoroughly. As is shown by previous experimental results, β-hairpin formation is initially driven by the bending propensity of the turn segment (Ji and Zhang 2008; Lewandowska et al. 2010; Munoz et al. 1997).

Figure 8b is the radius of gyration of the hydrophobic core. The resemblance between (a) and (b) indicates that

Table 1 Average backbone dihedral angles of folded and unfolded state

	Folded state	Unfolded state
Pro 4 Φ	−75°	−150°
Pro 4 Ψ	−25°	150°
Glu 5 Φ	−100°	−150°
Glu 5 Ψ	−50°	150°
Thr 6 Ψ	−15°	180°
Thr 8 Φ	−100°	100°
Thr 8 Ψ	150°	0°
Trp 9 Ψ	125°	0°

Other backbone dihedral angles have no obvious differences between the two states

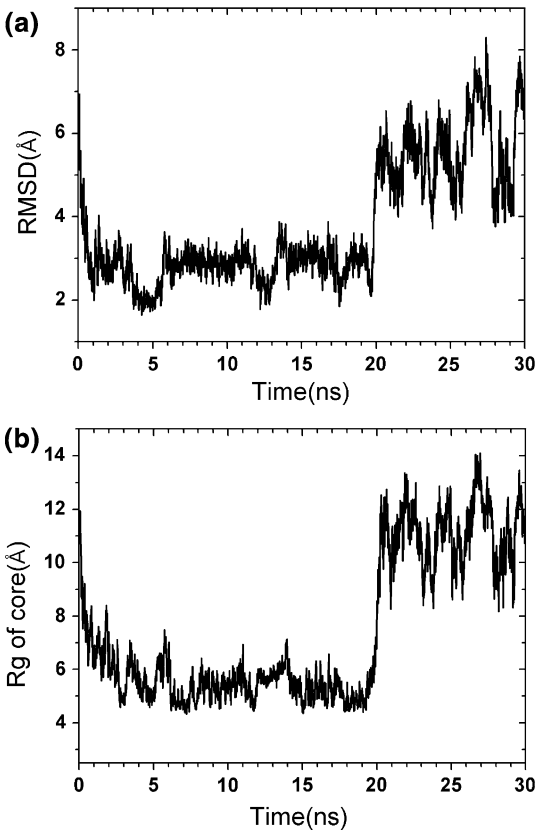

Fig. 8 Refolding of CLN025. **a** The RMSD of MD structures from crystal structure. **b** The Rg of the hydrophobic core. The resemblance between **a** and **b** indicates that the main driving force behind protein structure formation is hydrophobic interactions

the main driving force behind protein structure formation is hydrophobic interactions. The number of hydrogen bonds during the refolding simulation is far smaller than that in the equilibration simulation, so there is no evidence that the formation of hydrogen bonds between backbone peptide groups plays any significant role in the initial stage of folding.

We calculate the evolution of backbone dihedral angles during refolding, just like what we have done during unfolding. Whether in folded or unfolded state, Thr 6 Φ is about 75°. But in our refolding simulation, it is trapped in −100°. Tyr1 Φ and Tyr2 Ψ encounter the same situation. Tyr1 Φ is trapped in 50°, while it varies between −50°and −150° in folded/unfolded state. And Tyr2 Ψ is trapped in 25°, while it is about 150° in folded/unfolded state. That is to say, the β-hairpin is misfolded. The misfolded state is not stable and soon stretches to unfolded state (Fig. 9), and it will take a long time for these three angles to find the right answers.

Conclusion

In summary, molecular simulations are performed to study unfolding and refolding process of CLN025, a 10-residue β-hairpin. CLN025 is mainly stabilized by electrostatic interaction between the charged termini, so when it is pulled along the termini, the β-hairpin can unfold easily without large barrier. It is characterized by the force's fluctuation between negative and positive values not long after the beginning of simulation. Without water, interaction between termini is strengthened, and then the unfolding process is harder. Different from pulling along the termini, pulling along middle residues have two peaks. The first force peak indicates the resistance of hydrogen bonds and the second one represents the resistance of hydrophobic core. They share something too. In both conditions, the β-hairpin unfolds slower in vacuum than in aqueous solution. And their final backbone dihedral angles are the same, which is in accord with the two-state folding model. Moreover, in refolding process, the resemblance between profile of RMSD and Rg' evolution indicates that the main driving force behind protein structure formation is hydrophobic interactions. The collapse to β-hairpin-like conformations is very fast, with only 3.6 ns. But it is a misfolded state rather than a folded state. The misfolded state is not stable and soon stretches to unfolded state. And it is time-consuming for Tyr1 Φ, Tyr2 Ψ and Thr 6 Φ to go back to the right path. The simulation improves our understanding of this kind of miniprotein. It helps us investigate how large the area of ideal proteins is, whereas the sequence space of a 10-residue polypeptide is relatively limited and easier to be explored than naturally occurring proteins.

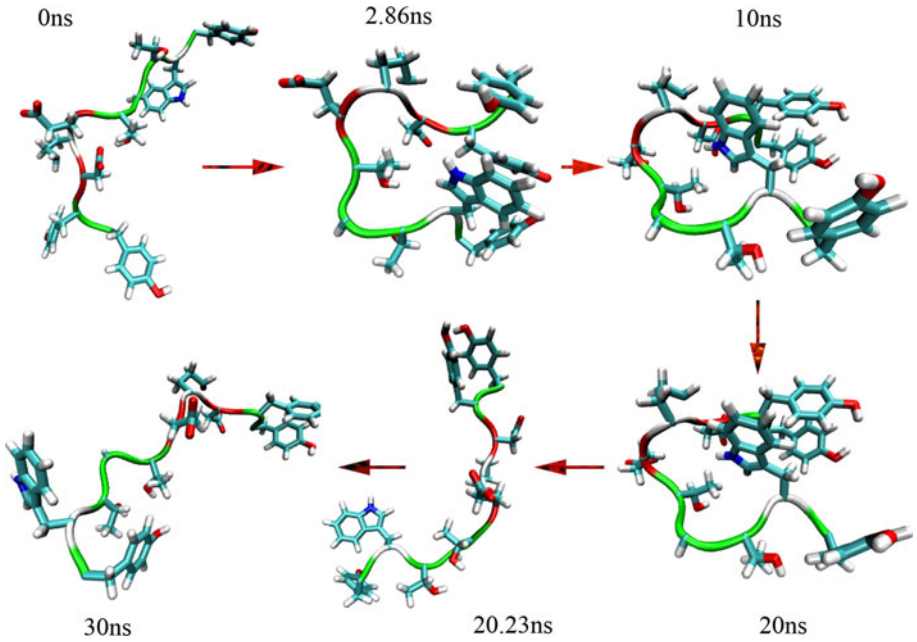

Fig. 9 Refolding snapshots of CLN025. The collapse to β-hairpin-like conformations is very fast, with only 3.6 ns. But it is a misfolded state rather than a folded state. The misfolded state is not stable and soon stretches to unfolded state

Acknowledgments This work was supported by NSFC (Nos. 20903094 and 20833008) and NKBRSF (Nos. 2007CB815202 and 2009CB220010) and 863 project (Nos. 2006AA01A119 and 2009AA01A130). GJZ also acknowledges financial support from Chinese Academy of Sciences for CAS-leader-prize winners and young scientists.

References

Alhambra C, Corchado JC, Sanchez ML, Gao JL, Truhlar DG (2000) Quantum dynamics of hydride transfer in enzyme catalysis. J Am Chem Soc 122:8197–8203

Best RB, Brockwell DJ, Toca-Herrera JL, Blake AW, Smith DA, Radford SE, Clarke J (2003) Force mode atomic force microscopy as a tool for protein folding studies. Anal Chim Acta 479:87–105

Bryant Z, Pande VS, Rokhsar DS (2000) Mechanical unfolding of a beta-hairpin using molecular dynamics. Biophys J 78:584–589

Cattani-Scholz A, Renner C, Cabrele C, Behrendt R, Oesterheld D, Moroder L (2002) Photoresponsive cyclic bis(cysteinyl)peptides as catalysts of oxidative protein folding. Angew Chem Int Ed Engl 41:289–292

Chen ZZ, Lou JZ, Zhu C, Schulten K (2008) Flow-induced structural transition in the beta-switch region of glycoprotein Ib. Biophys J 95:1303–1313

Chen J, Rempel DL, Gross ML (2010) Temperature Jump and Fast Photochemical Oxidation Probe Submillisecond Protein Folding. J Am Chem Soc 132:15502–15504

Cramer CJ, Truhlar DG (1999) Quantum and molecular dynamics study for binding of macrocyclic inhibitors to human alpha-thrombin. Chem Rev 99:2161–2200

Daniel RM, Dunn RV, Finney JL, Smith JC (2003) The role of dynamics in enzyme activity. Annu Rev Biophys Biomol Struct 32:69–92

Das A, Mukhopadhyay C (2009) Mechanical unfolding pathway and origin of mechanical stability of proteins of ubiquitin family: an investigation by steered molecular dynamics simulation. Proteins 75:1024–1034

Du DG, Zhu YJ, Huang CY, Gai F (2004) Understanding the key factors that control the rate of beta-hairpin folding. Proc Natl Acad Sci USA 101:15915–15920

Duan LL, Mei Y, Zhang DW, Zhang QG, Zhang JZH (2010) Folding of a Helix at Room Temperature Is Critically Aided by Electrostatic Polarization of Intraprotein Hydrogen Bonds. J Am Chem Soc 132:11159–11164

Eyles SJ, Kaltashov IA (2004) Methods to study protein dynamics and folding by mass spectrometry. Methods 34:88–99

Freddolino PL, Harrison CB, Liu YX, Schulten K (2010) Challenges in protein-folding simulations. Nature Phys 6:751–758

Ganim Z, Chung HS, Smith AW, DeFlores LP, Jones KC, Tokmakoff A (2008) Amide I two-dimensional infrared Spectroscopy of proteins. Acc Chem Res 41:432–441

Gao JL, Truhlar DG (2002) Quantum mechanical methods for enzyme kinetics. Annu Rev Phys Chem 53:467–505

Gao JL, Ma SH, Major DT, Nam K, Pu JZ, Truhlar DG (2006) Mechanisms and free energies of enzymatic reactions. Chem Rev 106:3188–3209

George DR, Patrick JF, Jayanth RB, Amos M (2006) A backbone-based theory of protein folding. Proc Natl Acad Sci USA 103:16623–16633

Golonzka O, Khalil M, Demirdöven N, Tokmakoff A (2001) Vibrational anharmonicities revealed by coherent two-dimensional infrared spectroscopy. Phys Rev Lett 86:2154–2157

Gruebele M (2010) Analytical biochemistry: weighing up protein folding. Nature 468:640–641

Guo C, Levine H, Kessler DA (2000) How does a beta-hairpin fold/unfold? Competition between topology and heterogeneity in a solvable model. Proc Natl Acad Sci USA 97:10775–10779

Guzmán DL, Roland JT, Keer H, Kong YP, Ritz T, Yee A, Guan Z (2008) Using steered molecular dynamics simulations and single-molecule force spectroscopy to guide the rational design of biomimetic modular polymeric materials. Polymer 49:3892–3901

Guzmán DL, Randall A, Baldi P, Guan ZB (2009) Haploinsufficiency for Pten and Serotonin transporter cooperatively influences brain

size and social behavior. Proc Natl Acad Sci USA 107:1989–1994
Hamdi M, Ferreira A, Sharma G, Mavroidis C (2008) Prototyping bio-nanorobots using molecular dynamics simulation and virtual reality. Microelectron J 39:190–201
Hatfield MPD, Murphy RF, Lovas SJ (2010) Molecular dynamics analysis of the conformations of beta-hairpin miniprotein. Phys Chem B 114:3028–3037
Honda S, Akiba T, Kato YS, Sawada Y, Sekijima M, Ishimura M, Ooishi A, Watanabe H, Odahara T, Harata K (2008) Crystal structure of a ten-amino acid protein. J Am Chem Soc 130:15327–15331
Huang X-Q, Zheng F, Zhan C-G (2008) Modeling Differential Binding of alpha 4 beta 2 Nicotinic Acetylcholine Receptor with Agonists and Antagonists. J Am Chem Soc 130:16691–16696
Hughes RM, Waters ML (2006) Model systems for beta-hairpins and beta-sheets. Curr Opin Struct Biol 16:514–524
Humphrey W, Dalke A, Schulten K (1996) VMD: visual molecular dynamics. J Mol Graph 14.1:33–38
Hunt NT (2009) 2D-IR spectroscopy: ultrafast insights into biomolecule structure and function. Chem Soc Rev 38:1837–1848
Ji CG, Zhang JZH (2008) Protein polarization is critical to stabilizing AF-2 and helix-2' domains in ligand binding to PPAR-gamma. J Am Chem Soc 130:17129–17133
Klimov DK, Newfield D, Thirumalai D (2002) Simulations of beta-hairpin folding confined to spherical pores using distributed computing. Proc Natl Acad Sci USA 99:8019–8024
Kolano C, Helbing J, Kozinski M, Sander W, Hamm P (2006) Watching hydrogen-bond dynamics in a beta-turn by transient two-dimensional infrared spectroscopy. Nature 444:469–472
Lewandowska A, Ołdziej S, Liwo A, Scheraga HA (2010) Beta-hairpin-forming peptides; models of early stages of protein folding. Biophys Chem 151:1–9
Li H, Cao EH, Gisler T (2009) Force-induced unfolding of human telomeric G-quadruplex: a steered molecular dynamics simulation study. Biochem Biophys Res Commun 379:70–75
Li JY, Fernandezb JM, Bernea BJ (2010) Water's role in the force-induced unfolding of ubiquitin. Proc Natl Acad Sci USA 107:19284–19289
Lim BBC, Lee EH, Sotomayor M, Schulten K (2008) Molecular basis of fibrin clot elasticity. Structure 16:449–459
Liu J-J, Hamza A, Zhan C-G (2009) Fundamental reaction mechanism and free energy profile for (−)-cocaine hydrolysis catalyzed by cocaine esterase. J Am Chem Soc 131:11964–11975
Lu H, Schulten K (1999) Steered molecular dynamics simulation of conformational changes of immunoglobulin domain I27 interpret atomic force microscopy observations. Chem Phys 247:141–153
Lu H, Schulten K (2000) The key event in force-induced unfolding of titin's immunoglobulin domains. Biophys J 79:51–65
Munoz V, Thompson PA, Hofrichter J, Eaton WA (1997) Folding dynamics and mechanism of beta-hairpin formation. Nature 390:196–199
Munoz V, Ghirlando R, Blanco FJ, Jas GS, Hofrichter J, Eaton WA (2006) Folding and aggregation kinetics of a beta-hairpin. Biochemistry 45:7023–7035
Nguyen PH, Stock G (2006) Nonequilibrium molecular dynamics simulation of a photoswitchable peptide. Chem Phys 323:36–44
Olsen S, Smith SC (2007) Radiationless decay of red fluorescent protein chromophore models via twisted intramolecular charge-transfer states. J Am Chem Soc 129:2054–2065
Olsen S, Smith SC (2008) Bond selection in the photoisomerization reaction of anionic green fluorescent protein and kindling fluorescent protein chromophore models. J Am Chem Soc 130:8677–8689
Pan JX, Han J, Borchers CH, Konermann L (2010) Characterizing Short-Lived Protein Folding Intermediates by Top-Down Hydrogen Exchange Mass Spectrometry. Anal Chem 82:8591–8597
Phillips JC, Braun R, Wang W, Gumbart J, Tajkhorshid E, Villa E, Chipot C, Skeel RD, Kalé L, Schulten KJ (2005) Scalable molecular dynamics with NAMD. Comput Chem 25:1781–1802
Pineda JR, Callender R, Schwartz SD (2007) Ligand binding and protein dynamics in lactate dehydrogenase. Biophys J 93:1474–1483
Renner C, Behrendt R, Spörlein S, Wachtveitl J, Moroder L (2000a) Photomodulation of conformational states. I. Mono- and bicyclic peptides with (4-amino)phenylazobenzoic acid as backbone constituent. Biopolymers 54:489–500
Renner C, Cramer J, Behrendt R, Moroder L (2000b) Photomodulation of conformational states. II. Mono- and bicyclic peptides with (4-aminomethyl)phenylazobenzoic acid as backbone constituent. Biopolymers 54:501–514
Rhee YM, Sorin EJ, Jayachandran G, Lindahl E, Pande VS (2004) Simulations of the role of water in the protein-folding mechanism. Proc Natl Acad Sci USA 101:6456–6461
Rief M, Oesterhelt F, Heymann B, Gaub HE (1997) Single molecule force spectroscopy on polysaccharides by atomic force microscopy. Science 275:1295–1297
Riemen AJ, Waters ML (2010) Dueling post-translational modifications trigger folding and unfolding of a beta-hairpin peptide. J Am Chem Soc 132:9007–9013
Saen-Oon S, Ghanem M, Schramm VL, Schwartz SD (2008) Remote mutations and active site dynamics correlate with catalytic properties of purine nucleoside phosphorylase. Biophys J 94:4078–4088
Selkoe DJ (2003) Folding proteins in fatal ways. Nature 426:900–904
Shank EA, Cecconi C, Dill JW, Marqusee S, Bustamante C (2010) The folding cooperativity of a protein is controlled by its chain topology. Nature 465:637–641
Shelimov KB, Clemmer DE, Hudgins RR, Jarrold MF (1997) Protein structure in vacuo: gas-phase confirmations of BPTI and cytochrome c. J Am Chem Soc 119:2240–2248
Sotomayor M, Schulten K (2007) Single-molecule experiments in vitro and in silico. Science 316:1144–1148
Spörlein S, Carstens H, Satzger H, Renner C, Behrendt R, Moroder L, Tavan P, Zinth W, Josef W (2002) Ultrafast spectroscopy reveals subnanosecond peptide conformational dynamics and validates molecular dynamics simulation. Proc Natl Acad Sci USA 99:7998–8002
Tsui V, Garcia C, Cavagnero S, Siuzdak G, Dyson HJ, Wright PE (1999) Quench-flow experiments combined with mass spectrometry show apomyoglobin folds through an obligatory intermediate. Protein Sci 8:45–49
Wu EL, Mei Y, Han KL, Zhang JZH (2007) Photochemistry of aryl halides: photodissociation dynamics. Biophys J 92:4244–4253
Yang MJ, Zhang X, Han KL (2010) Molecular dynamics simulation of SRP GTPases: towards an understanding of the complex formation from equilibrium fluctuations. Proteins Struct Funct Bioinform 78:2222–2237
Yang MJ, Pang XQ, Zhang X, Han KLJ (2011) Molecular dynamics simulation reveals preorganization of the chloroplast FtsY towards complex formation induced by GTP binding. Struct Biol 173:57–66
Zeng XC, Hu H, Zhou HX, Marszalek PE, Yang WT (2010) Equilibrium sampling for biomolecules under mechanical tension. Biophys J 98:733–740
Zhao P-L, Wang L, Zhu X-L, Huang X-Q, Zhan C-G, Wu J-W, Yang G-F (2010) Subnanomolar Inhibitor of cytochrome bc(1) complex designed by optimizing interaction with conformationally flexible residues. J Am Chem Soc 132:185–194
Zhou RH, Berne BJ (2002) Can a continuum solvent model reproduce the free energy landscape of a beta-hairpin folding in water? Proc Natl Acad Sci USA 99:12777–12782
Zwanzig R (1997) Two-state models of protein folding kinetics. Proc Natl Acad Sci USA 94:148–150